

# We are IntechOpen, the world's leading publisher of Open Access books Built by scientists, for scientists

6,900

Open access books available

186,000

International authors and editors

200M

Downloads

Our authors are among the

154

Countries delivered to

TOP 1%

most cited scientists

12.2%

Contributors from top 500 universities



WEB OF SCIENCE™

Selection of our books indexed in the Book Citation Index  
in Web of Science™ Core Collection (BKCI)

Interested in publishing with us?  
Contact [book.department@intechopen.com](mailto:book.department@intechopen.com)

Numbers displayed above are based on latest data collected.  
For more information visit [www.intechopen.com](http://www.intechopen.com)



# Frequency Dependent Specialization for Processing Binaural Auditory Cues in Avian Sound Localization Circuits

Rei Yamada and Harunori Ohmori  
Kyoto University  
Japan

## 1. Introduction

Localizing sound sources is essential for survival of animals. It enables animals to avoid danger, or to catch their prey. The differences of sound information between two ears, those of interaural time and level difference (ITD and ILD), are important cues for sound source localization. The minimum resolvable angle of sound source separation is less than  $30^\circ$  along the horizontal plane in many species (cat, Casseday & Neff, 1973; rat, Masterton et al., 1975; songbirds, Klump et al., 1986; Park & Dooling, 1991; Klump, 2000), and in some species the resolution is extremely high. In human and in barn owl, the resolvable angle is as small as  $1^\circ$  (Mills, 1958; Knudsen & Konishi, 1979). ITD and ILD cues depend on the head size of animals and are quite small, particularly in small-headed animals. Thus processing of these cues may need specialization of individual neurons and neural circuits. The time and level information of sounds are captured in the cochlea, transformed to trains of action potentials in the auditory nerve fibers, and then transmitted to auditory nuclei in the brainstem. In the brainstem, time and level information are extracted in the cochlear nucleus and then transmitted in parallel pathways which are specialized to process ITD and ILD cues separately (Fig. 1A, indicating the auditory brainstem circuit in birds) (Sullivan & Konishi, 1984; Takahashi et al., 1984; Takahashi & Konishi, 1988; Warchol & Dallos, 1990; Moiseff & Konishi, 1983; Yin, 2002). Furthermore, in the auditory system, neurons are tuned to a specific frequency of sound (characteristic frequency, CF), and ITD and ILD cues are processed by each CF neuron (Brugge, 1992; Klump, 2000). Recently, a series of studies in the chicken have revealed several frequency dependent specializations in ITD coding pathway (Kuba et al., 2005; Yamada et al., 2005; Kuba et al., 2006). These specializations include the type and the density of ion channels, and their subcellular localization. Furthermore, recent observations in mammals and birds indicate that time and level information are not processed independently but rather cooperatively to enhance the contrast of interaural difference cues even at the first stage of processing of these cues in the brainstem auditory nuclei (Brand et al., 2002; Nishino et al., 2008; Sato et al., 2010). In this chapter, we will first summarize what is known about the neural specializations that enable the preciseness of coincidence detection of synaptic inputs, which is central to process the ITD. And then, we will review observations on how the interaction of time and level information of sounds modulates the processing of each ITD and ILD cue.

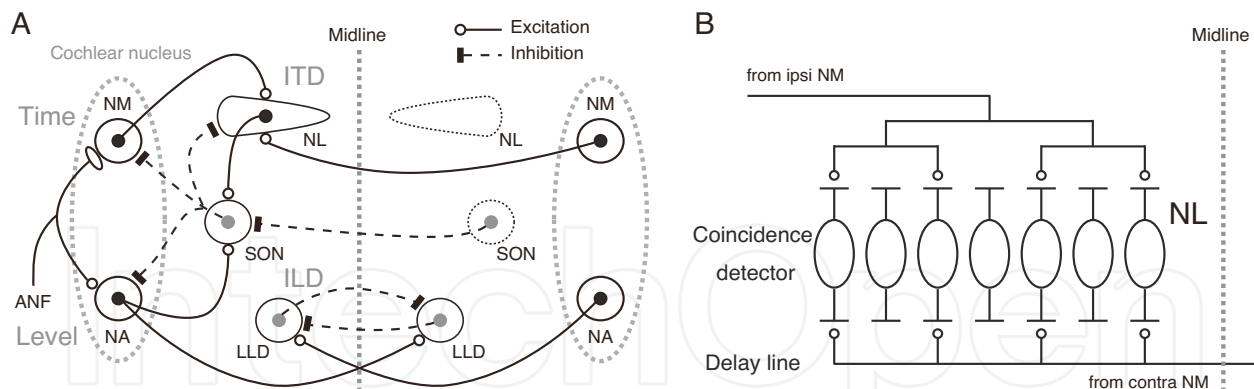


Fig. 1. (A) Schematic diagrams of the auditory brainstem circuits for processing ITD and ILD in birds. (B) Modification of Jeffress model incorporating features of NL of the chick. The contralateral projections from NM to NL form delay lines, while NL neurons act as coincidence detectors of bilateral excitatory inputs. When the sound source moves toward more contralateral locations, spikes from contralateral NM will arrive at NL faster, and bilateral spikes arrive simultaneously at the NL neuron located more laterally.

## 2. Specialization of ITD coding neurons

Extraction of ITDs in birds is explained on the classical Jeffress model (Jeffress, 1948), which requires delay lines and an array of coincidence detectors (Fig. 1B). Delay lines delay the arrival time of action potential to the coincidence detectors, while the coincidence detectors fire maximally when they receive synaptic inputs simultaneously from both ears. These two elements allow each ITD to be encoded as the place of neuron in the neuronal array. In birds, ITDs are processed in the nucleus laminaris (NL, Fig. 1A) (Konishi, 2003), which is a homologue of the mammalian nucleus of the medial superior olive (MSO). NL is innervated bilaterally from the nucleus magnocellularis (NM). NM extracts fine temporal information of sounds from auditory nerve fibers. In the chicken, the projection fibers from contralateral NM to NL form delay lines (Young & Rubel, 1983; Carr & Konishi, 1988), while NL neurons act as coincidence detectors of bilateral synaptic inputs (Fig. 1B) (Carr & Konishi, 1990; Overholt et al., 1992). Sensitivity to ITDs is extremely high in NL neurons. *In vivo* single-unit studies in the barn owl NL showed that the half-peak width of the ITD tuning curve varies with the CF of neurons, and reaches about 0.1-0.2 ms at 3-7 kHz (Carr & Konishi, 1990; Fujita & Konishi, 1991). This sharpness of ITD tuning of NL neurons should underlie the resolution of a microsecond order of ITDs in the barn owl (Moiseff & Konishi, 1981) and should be determined by the coincidence detection of NL neurons. The cellular mechanism of coincidence detection in NL neurons was studied *in vitro* (Kuba et al., 2003). Experiments were made in brainstem slices of the posthatch chick of P3-P11 at the body temperature of birds (40°C). Under the whole-cell recording, EPSPs were evoked in NL neurons by electrical stimuli applied to both sides of projection fibers from NM, while the time interval between the two stimuli ( $\Delta t$ ) was varied (Fig. 2A). The EPSPs were summated to generate an action potential as the interval of two stimuli decreased. The probability of firings peaked at  $\Delta t$  of 0 ms (Fig. 2A and B), and the half-peak width of the coincidence detection curve (time window) was 0.4 ms (Fig. 2B), which is comparable to that observed in the barn owl NL *in vivo* (Carr & Konishi, 1990). What cellular mechanisms underlie to achieve such a high accuracy of coincidence detection?

The acceleration of EPSP time course is essential for the accurate coincidence detection (Kuba et al., 2003) by limiting the time window for the summation of bilateral EPSPs. NL neurons reduce their input resistance extensively by activating several membrane conductances at the resting membrane potential (Reyes et al., 1996; Trussell, 1999; Kuba et al., 2002; Kuba et al., 2003). Among them, the most important is the conductance of low-threshold  $K^+$  current ( $I_{KLT}$ ).  $I_{KLT}$  is mediated by subtypes of voltage-gated  $K^+$  channels, Kv1.1 and 1.2, and in particular, Kv1.2 channels are predominant in the NL (Fukui & Ohmori, 2004; Kuba et al., 2005). Developmentally,  $I_{KLT}$  increases nearly fourfold around the hatch, and becomes the dominant conductance at resting potential in NL neurons (Kuba et al.,

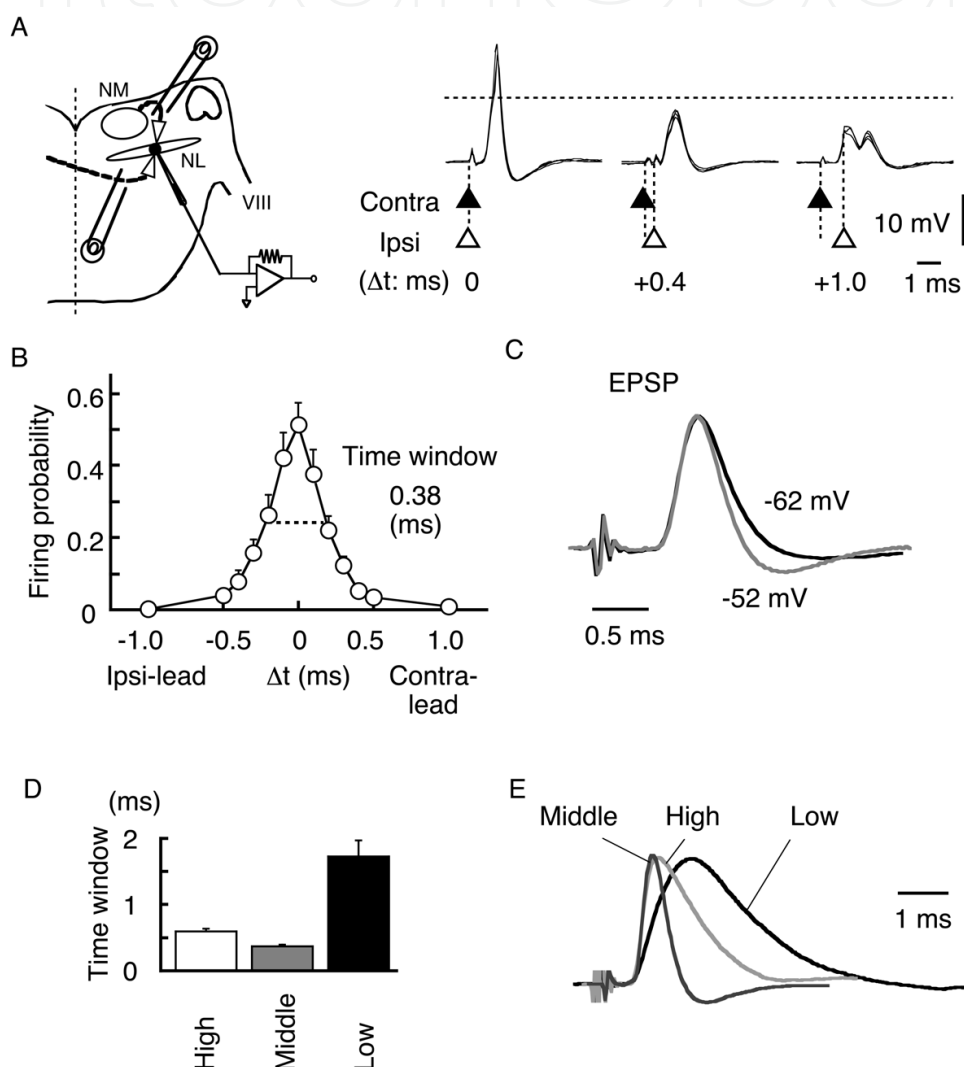


Fig. 2. Rapid EPSP time course is essential for coincidence detection (from Kuba et al., 2003; Kuba et al., 2005). (A) Bilateral EPSPs are evoked at different time intervals ( $\Delta t$ ). Spikes are generated when  $\Delta t$  is small. (B) Probability of spike generation as a function of  $\Delta t$ . The time window is indicated by the horizontal broken line. (C) EPSPs from the same NL neurons at different holding potentials. EPSP is accelerated with membrane depolarization (from -62 to -52 mV). Data are from middle CF neurons. (D) Time window of coincidence detection at each CF. (E) EPSPs from each CF are normalized and superimposed. EPSP is fastest and coincidence detection is the most accurate at middle CF.

2002). Moreover, it is activated near the resting membrane potential with rapid kinetics ( $-60$  mV; Rathouz & Trussell, 1998).  $I_{\text{KLT}}$  is activated by a small membrane depolarization and accelerates the falling phase of EPSP. Consequently, EPSP has a fast time course as fast as EPSC at the resting membrane potential, and is even faster than EPSC with a small membrane depolarization (Fig. 2C). These findings indicate that  $I_{\text{KLT}}$  plays a crucial role in shortening the time window of coincidence detection to submillisecond order. Recently, a similar developmental increase of  $I_{\text{KLT}}$  has been reported to shape the EPSPs in the mammalian MSO neurons (Scott et al., 2005).

### 3. Frequency specific expression of $I_{\text{KLT}}$

Although the range of audible frequencies varies among species, precision is the highest in the middle frequencies in most avian species; thus the acuity of azimuthal sound source localization depends on the sound frequency (Klump, 2000). NL is organized tonotopically; the CF of neurons is high in the rostral-medial (high CF) NL and decreases monotonically to the caudo-lateral (low CF) NL (Rubel & Parks, 1975). ITDs are determined separately by frequency-specific NL neurons. The coincidence detection is dependent on the frequency region of NL (Kuba et al., 2005), and their time window of coincidence detection was the smallest at the middle CF neurons, closely followed by the high CF neurons, and was the largest at the low CF neurons (Fig. 2D). Thus the acuity of coincidence detection is the highest in the middle CF NL neurons.

The EPSP time course is the fastest in the middle CF NL neurons (Fig. 2E). The size of  $I_{\text{KLT}}$  conductance is the largest at the middle CF. The expression of Kv1.2 channels is the highest in the middle CF neurons, followed by the high CF neurons, and is the lowest in the low CF neurons (Kuba et al., 2005). These observations indicate that the high level of Kv1.2 expression accelerates the EPSPs and determines the tonotopy of the coincidence detection in NL. Thus, the dominant expression of Kv1.2 may underlie the high resolution of sound localization in the middle frequency range in avian species (Klump, 2000).

### 4. HCN channel

Hyperpolarization-activated cation current ( $I_h$ ) is another major conductance activated at the resting membrane potential in NL neurons (Kuba et al., 2002).  $I_h$  has slow activation and deactivation kinetics, and has the reversal potential positive to the resting membrane potential ( $-50$  to  $-20$  mV) (Pape, 1996). These allow  $I_h$  to accelerate the EPSPs in two ways. First, it works as a shunting conductance to shorten the membrane time constant. Second, it depolarizes the resting membrane potential and activates  $I_{\text{KLT}}$ . Thus,  $I_h$  contributes to improve the coincidence detection.

$I_h$  is mediated by HCN (hyperpolarization-activated and cyclic nucleotide-gated) channels and four channel subtypes have been described (HCN1 ~ 4) with different rates of activation and different sensitivities to cyclic nucleotides (Santoro & Tibbs, 1999). Expressions of HCN1 and HCN2 are demonstrated in NL neurons and the level of expression varies along the tonotopic axis (Yamada et al., 2005). HCN1 is expressed highest at the low CF and decreases toward the high CF NL region, while HCN2 is evenly distributed along the tonotopic axis. What is the functional significance of this CF-dependent expression of HCN channels? HCN1 channels have a more positive activation voltage than HCN2 channels (Santoro & Tibbs, 1999). Because of the predominant expression of HCN1 channels,  $I_h$



conductance shortens the membrane time constant and improves the coincidence detection in the middle-low CF NL neurons. In contrast in high CF neurons, the  $I_h$  conductance is rather small at the resting potential because HCN2 channels are activated at more negative membrane potentials than the resting level. HCN2 channels are more sensitive to  $[cAMP]_i$  than HCN1 channels are, and the increase of  $[cAMP]_i$  shifts the voltage-dependence of activation to a positive direction (Ludwig et al, 1998; Santoro et al., 1998; Santoro & Tibbs, 1999). This makes it possible for the high CF neurons to increase the  $I_h$  conductance at the resting potential through the elevation of  $[cAMP]_i$  (Fig. 3A) (Yamada et al., 2005). Monoamine or acetylcholine is known to modulate  $I_h$  by regulating  $[cAMP]_i$  (DiFrancesco et al., 1986; DiFrancesco & Tromba, 1988a,b; Bobker & Williams, 1989). In NL, noradrenaline elevates  $[cAMP]_i$  and increases the  $I_h$  conductance, depolarizes the membrane and accelerates the EPSPs (Fig. 3B). Thus, the acuity of coincidence detection is enhanced by noradrenaline via the modulation of  $I_h$  in the high CF neurons (Fig. 3C). A small depolarization of the membrane by the current injection enhanced the coincidence detection almost to the same extent as that caused by depolarization by noradrenaline. This indicates that the noradrenergic effect on the coincidence detection is mediated by the membrane depolarization through the activation of  $I_{KLT}$  conductance.

These results raise the possibility that coincidence detection is under sympathetic control. An interesting observation was made in the barn owl (Knudsen & Konishi, 1979). The accuracy of sound source localization was tested by using either a short sound of 75 ms long or a long sound of 1 s long. There was no difference in the error of localization at the initial stage of head orientation whether the test sound stimulus was short or long and whether the sound was a broadband noise or a pure tone; perhaps barn owl measures the ITD at the onset of sound. However, adjustment of the head orientation at the end of a long sound stimulus clearly improved in the middle-high CF ranges (6-8 kHz) (Figure 3 of Knudsen & Konishi, 1979). This improvement might be related to the sympathetic activity when the

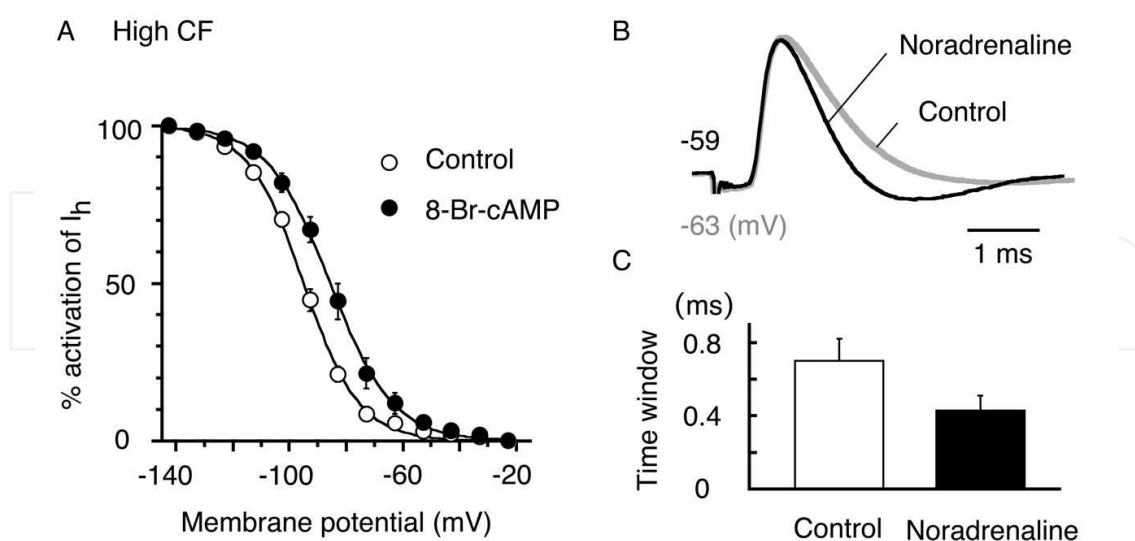


Fig. 3. Enhancement of coincidence detection by noradrenaline at high CF NL neurons (from Yamada et al., 2005). (A) Voltage-dependent activation curve of  $I_h$  at high CF. Membrane permeable analogue of cAMP (8-Br-cAMP) shifts the voltage dependence of  $I_h$  positively (filled circles). Noradrenaline depolarized the membrane potential, accelerates EPSP (B), and improves coincidence detection (C) at high CF.

animal was exposed to a long sound stimulus. However, the expression pattern of HCN channel subunits has not been examined in owls.

The CF-specific ITD information is integrated across frequencies at higher order nuclei to create an auditory space map (Konishi, 2003). Therefore, the noradrenergic enhancement of coincidence detection in the high CF NL neurons should increase the resolution of sound source localization. Neurons in the nucleus locus ceruleus send noradrenergic projections to almost all regions of the brain (Jones & Moore, 1977), and activities of these neurons are increased during a high arousal state (Aston-Jones & Bloom, 1981). This may suggest that noradrenergic systems are effective to increase the resolution of sound localization when animals are listening carefully to the sounds.

### 5. Specialization of action potential initiation site along the tonotopic axis

NL neurons are also specialized along the tonotopic axis in initiating action potentials in the axon. The axon initial segment has a high density of Nav channels (Catterall, 1981), and is the site of action potential initiation in many neurons (Mainen et al., 1995; Luscher & Larkum, 1998). However, the electron-microscopic studies indicated that the axon initial segment of NL neurons is myelinated in the chicken and the barn owl (Carr & Boudreau, 1993). Since the myelination was not observed in low-frequency NL neurons (below 1 kHz), they considered that the myelinated initial segment could be a consequence of adaptation for accurate binaural processing of high frequency sounds. This raises questions as to the location and role of action potential initiation site in NL neurons.

The distribution of Nav channels was studied in NL of the chicken (Kuba et al., 2006), and found that Nav1.6 channels are expressed and clustered in the axon, while they are almost absent in the soma. The distribution is different tonotopically, and in the high CF neurons, the cluster of Nav1.6 channels is located at some distance from the soma (50  $\mu\text{m}$ ) and stretches a short segment of the axon (10  $\mu\text{m}$ ), while it is located closer to the soma (5  $\mu\text{m}$ ) and is extended much longer segment (25  $\mu\text{m}$ ) in the low CF neurons. Thus, the site of action potential initiation is displaced more distant from the soma as the CF of neurons becomes higher. Consistently, the somatic amplitude of action potentials is small in the high CF NL neurons.

The CF-specific distribution of Nav channels ensures the acuity of coincidence detection. In the high CF neurons, the higher rates of synaptic inputs temporally summate and generate a plateau depolarization at the soma. This depolarization inactivates Nav channels and impedes the generation of action potentials, and consequently reduces the ITD sensitivity of the neuron. A distant localization of Nav channels from the soma may reduce the level of depolarization and the level of inactivation electrotonically. A computer simulation predicted that a distant localization of Nav channels enables the processing of ITD with a high peak-trough contrast (the contrast of firing rate between the peak and trough of the ITD tuning curve) in the high CF neurons.

### 6. Sound level dependent inhibition modulates the ITD tuning in NL

Processing of ITDs in NL *in vivo* is affected by sound loudness. Loud sound was expected to reduce the peak-trough contrast by simulation (Dasika et al., 2005). However, the peak-trough contrast was maintained rather at high sound pressure level in the barn owl (Pena et al., 1996). They proposed that inhibition from the superior olivary nucleus (SON) controls

ITD tuning in NL, rendering it tolerant to sound pressure level. The level information of sound is extracted in the nucleus angularis (NA), which is another subdivision of cochlear nucleus (Fig. 1A). The SON receives excitatory inputs from the NA and makes an inhibitory innervation to NA, NM, and NL in a sound-level-dependent manner (Lachica et al., 1994; Yang et al., 1999; Monsivais et al., 2000; Burger et al., 2005; Fukui et al., 2010). By recording single unit activity in NL of chicken *in vivo*, the ITD tuning in NL is found being controlled by both the frequency and level of sounds (Nishino et al., 2008). In the following discussion, best frequency (BF) is used as an alternative to CF. BF is the sound frequency at which the neuron generates spikes at the highest rate, while CF is the frequency at which neurons are driven at the lowest level of sound.

The peak-trough contrast of ITD tuning in the low BF units (BF lower than 1 kHz) became larger as the sound became louder, and was maintained high even at the loudest sound levels (Fig. 4A). After electrical lesion of the SON, the peak-trough contrast of ITD tuning curve collapsed at loud sound levels in the low BF NL neurons (Fig. 4B). In contrast, the peak-trough contrast of the middle-high BF units (higher than 1 kHz) was maximized at the intermediate sound pressure level and was practically lost when a loud sound was applied, which was similar to that of the low BF units after the lesion of SON. Furthermore, the level dependence of peak-trough contrast of middle-high BF neurons was not different from the control after the lesion of SON. These observations demonstrated that the BF dependence of level-dependent ITD tuning reflects the BF dependence of SON control on NL. The pattern and density of the SON projection to NL is correlated with this BF dependent effect of the SON. The GABAergic projection from SON to NL is robust in the low BF region of the nucleus and is less prominent towards the high BF region (Nishino et al., 2008). Therefore, the dense inhibitory projection from SON to NL is concluded to regulate the ITD tuning in NL.

The computer simulation that is based on a NEURON model reproduced a level dependence of ITD tuning in NL neurons (Nishino et al., 2008). The simulation further showed that without balance in the bilateral excitation, the peak-trough contrast of ITD tuning lost tolerance to the loud sounds. The SON inhibition might also play a role in maintaining the balance of excitation from NM on the two sides (Dasika et al., 2005).

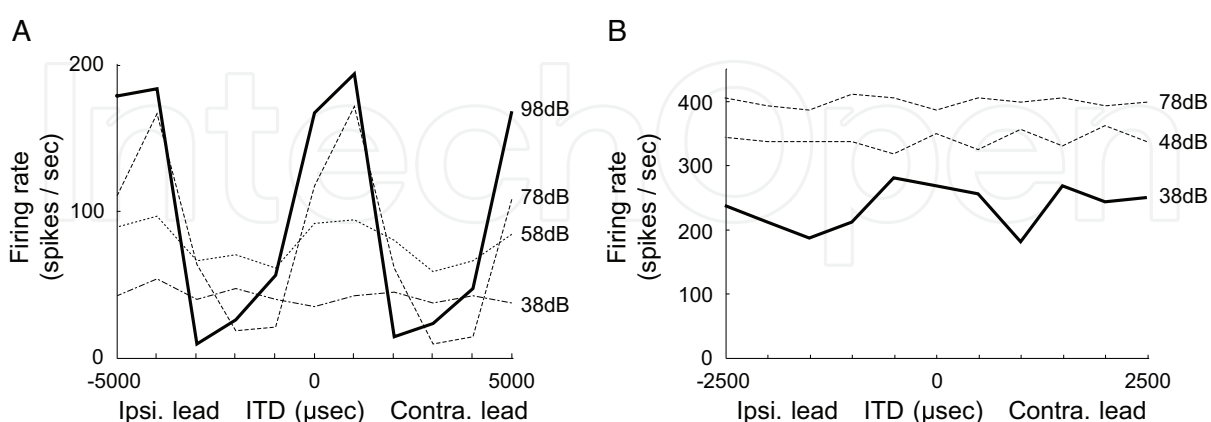


Fig. 4. ITD tuning to a pure-tone sound stimulus of low BF unit in NL (from Nishino et al., 2008). (A) ITD tuning curves from a low BF NL unit (200 Hz) with different sound pressure levels. The solid line indicates the ITD tuning curve of best peak-trough contrast. (B) ITD tuning curves from a low BF NL unit (400 Hz) after SON lesion.



## 7. ILD coding

In birds, the interaural level differences (ILDs) are processed in the dorsal lateral lemniscal neurons (LLD). The LLD receives excitatory inputs from the contralateral NA and inhibitory inputs from the ipsilateral NA via the contralateral LLD (Manley et al., 1988; Takahashi & Konishi, 1988; Mogdans & Knudsen, 1994; Konishi, 2003). Therefore, LLD neurons are excited by contralateral sound and inhibited by ipsilateral sound, and encode ILDs by comparing the sound level between two ears (Fig. 5A). However, small head diameter of the animal and the limited audible frequency range ( $< 4\text{kHz}$ ) may limit the physiological relevant range of ILD to about  $\pm 5\text{ dB}$  or narrower in the chicken. By recording single unit activity in NA and LLD of chicken *in vivo*, the neural activity in these neurons was found being affected by the interaural phase difference (IPD), which is a frequency-independent formula of ITD, through acoustic interference across the interaural canal that connects the middle ears of the two sides in birds (Sato et al., 2010).

The firing of the NA unit increased monotonically not only by the ipsilateral sound but also by the contralateral sound, whereas the sensitivity was lower (about  $15\text{ dB}$ ) with the contralateral sound. Activity in the NA is affected by strong contralateral sound through the interaural canal, an air-filled connection between the two middle ear cavities (Fig. 5A). During the binaural sound stimulus, the interaction of contralateral sound shows IPD dependence (Fig. 5B). Increasing the level of out-of-phase ( $\text{IPD} = 180^\circ$ ) contralateral sound monotonically increased the firing rate of the NA neurons, whereas increasing the in-phase ( $0^\circ$ ) sound produced a local minimum (dip-ILD) and then increased the firing rate, and the depth of the dip was affected by the IPD (Fig. 5B). According to the NA activity, the LLD unit is strongly modulated by the IPD. LLD neurons are activated by contralateral NA activity and are inhibited by ipsilateral NA activity. Therefore, the firing activity of LLD neurons is high at negative ILDs (ipsi  $<$  contra) and declines to positive ILDs (ipsi  $>$  contra). Fig. 5C shows a unit that exhibited a low firing rate when the sound level was not different in two ears. The firing activity was nearly absent at  $0\text{ dB}$  to positive ILDs, demonstrating a strong ipsilateral inhibition on this unit. Another unit (Fig. 5D) fired robust even when the sound to the ipsilateral ear was loud (positive ILDs). The ipsilateral inhibition may not be strong in this unit. The rate-ILD relationship varied with the IPD in both units, and the firing rate was lowest for the in-phase sound ( $0^\circ$  IPD, thick solid lines), and the rate increased in most cases when IPD was included, to some extent.

In the open field, any displacement of the sound source from the midline must cause a correlated change in both the level and phase of sounds between two ears. When the sound source is presented at the midline, the ILD is  $0\text{ dB}$  and IPD is  $0^\circ$ . A sound source displacement towards the contralateral ear generates negative ILD and positive IPD in the binaural sounds (by definition), and towards ipsilateral ear generates positive ILD and negative IPD (Fig. 5C and D). With any IPD, the firing rate of most units increases (Fig. 5C and D). Therefore, the responsiveness of the LLD units to small changes of ILD, namely the slope of rate-ILD relationship, is increased toward the contralateral ear (negative ILD) and decreases toward the ipsilateral ear (positive ILD) corresponding to the respective displacement of the sound source from the midline.

Consequently, the modulation of neuronal activity by IPD enhances the responsiveness of LLD neurons to the contralateral field. Any particular dependence of this enhancement on the BF was not found; however the sample numbers were small and most recordings were made in high-BF LLD units.

A simple model is proposed to explain the interaural coupling effects and IPD modulation of LLD activity (Sato et al., 2010), and concluded that the modulation of neuronal activity by IPD increases the sensitivity of LLD neurons to the contralateral field, and may improve the processing of small ILD cues.

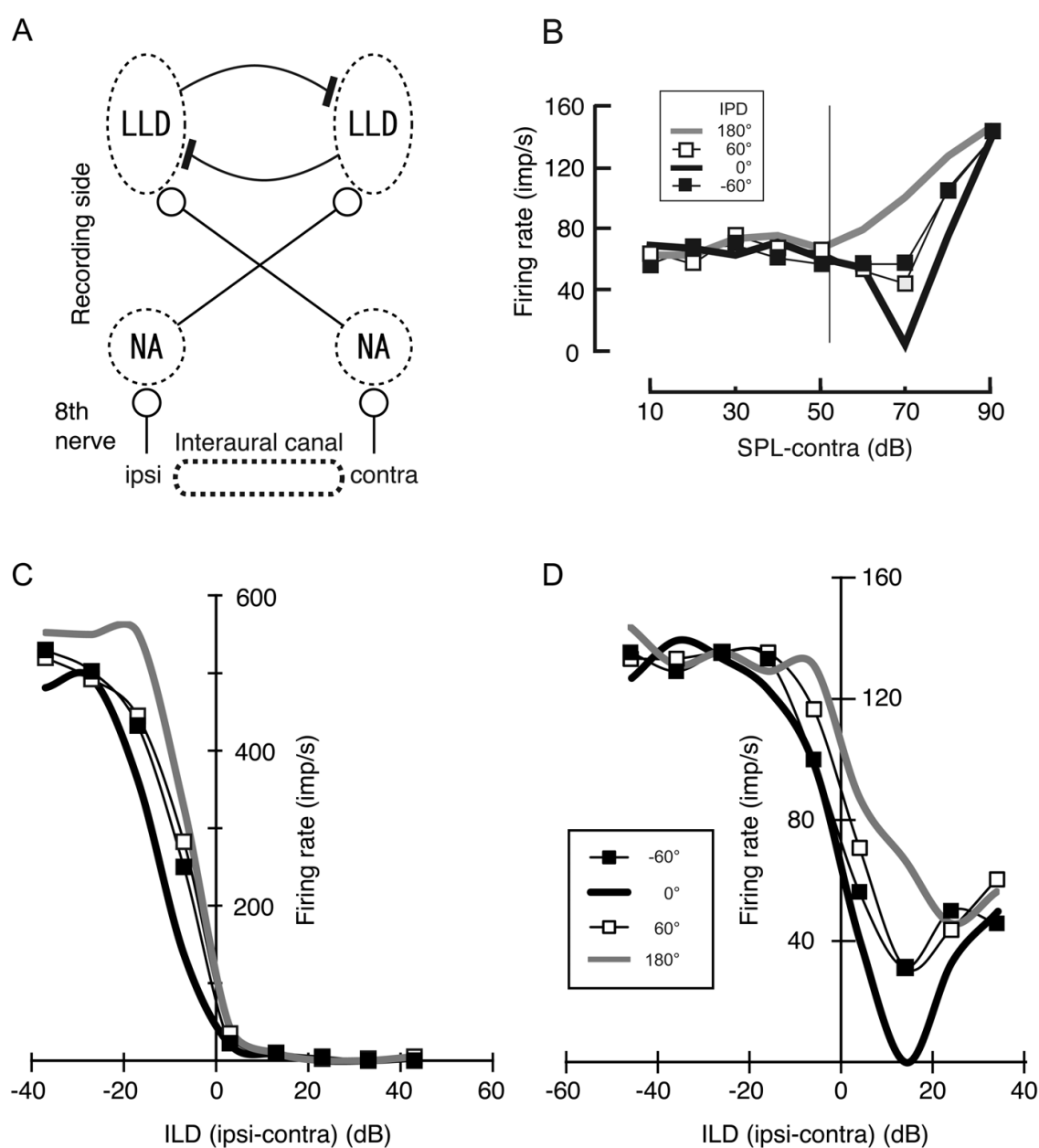


Fig. 5. IPD modulates the neural activity in the NA and LLD (from Sato et al., 2010). (A) Schematic diagrams to show the ILD processing circuit in the brainstem. Open circles indicate excitatory projections and filled bars indicate inhibitory projections. (B) The firing rate of NA unit (BF 200 Hz) as a function of contralateral sound pressure level (SPL). Ipsilateral sound (52 dB SPL) is constant at 20 dB above the threshold. A vertical thin line indicates the 0 ILD in this unit. Binaural sound is presented at four IPDs, as indicated by the different symbols. (C and D) IPD-dependence of rate-ILD relationship of two typical LLD units. The inset indicates IPDs applied to both (C) and (D).

## 8. Comparison to mammals

MSO neurons have several morphological and biophysical features common to NL neurons (Oertel, 1999; Trussell, 1999). These include bipolar dendrites (Scheibel & Scheibel, 1974), rapid time course of EPSCs (Smith et al., 2000), and large conductance of  $I_{KLT}$  and  $I_h$  (Smith, 1995; Svirskis et al., 2002). Furthermore, channel molecules underlying the synaptic and membrane conductances are also common between MSO and NL (Parks, 2000; Rosenberger et al., 2003; Koch et al., 2004), suggesting that the two structures share some common mechanisms for enhancing the coincidence detection of binaural excitatory inputs. However, no tonotopic specializations have been reported in the morphological and biophysical features in MSO. This might be related to the limited frequency range that mammals use for the ITD extraction (below 1.5 kHz; Heffner & Heffner, 1988). Nevertheless, more thorough studies need to be conducted in MSO along the tonotopic axis.

Single unit recordings from the MSO of gerbils revealed that glycinergic inhibition improved ITD processing for low-frequency sound (Brand et al., 2002). Suppression of inhibition by the iontophoretic application of strychnine increased the firing rate of MSO neurons and shifted the peak of ITD tuning curves from contralateral-leading ITD to 0 ITD. They concluded that precisely timed inhibition from the contralateral ear via the medial nucleus of the trapezoid body (MNTB) precedes the excitatory input from that side and creates an effective delay in the excitatory response, which is essential for ITD coding (Brand et al., 2002). The cell in MNTB is a relay neuron, which receives excitatory input from contralateral globular bushy cells in the anteroventral cochlear nucleus, and projects ipsilaterally to MSO and lateral superior olive (LSO) (Spangler et al., 1985; Adams & Mugnaini, 1990; Cant & Hyson, 1922). The MNTB neurons are also sensitive to the sound level (Tollin & Yin, 2005). In fact, the ITD tuning of MSO neurons could be maintained even at loud sound (Pecka et al., 2008). It has also been shown that the processing of ILD in LSO, which is a homologue of the LLD in birds, depends critically on timing; the timing of contralateral inhibition through MNTB has to be matched with ipsilateral excitation (Finlayson & Caspary, 1991; Smith et al., 1993; Joris & Yin, 1995; Tollin & Yin, 2005). These evidences suggest that also mammals may use the time and level information of sounds cooperatively to extract ITD and ILD cues.

## 9. Conclusion

We reviewed here how the ITD and ILD cues are precisely processed basing on the *in vitro* and *in vivo* researches conducted in the chicken auditory brainstem. In the ITD coding circuit, NL neurons show several functional as well as morphological refinements along the tonotopic axis to enhance the coincidence detection at each frequency. In particular, the expression of channel molecules is highly organized in NL neurons to regulate auditory coincidence detection across frequencies. We need to know further how the subcellular localization of these molecules contributes to the computation of neurons and also to the behavior of animals. In addition, new evidences suggest that time and level information of sounds are used not independently but rather cooperatively to improve the processing of both ITD and ILD cues. Interaural difference cues can be small, particularly for an animal with a small head. Both mammals and birds may use similar strategies to compensate the small interaural difference cues for the accurate sound source localization.

## 10. References

- Adams, J.C. & Mugnaini, E. (1990). Immunocytochemical evidence for inhibitory and disinhibitory circuits in the superior olive. *Hear. Res.*, 49, 281-298,
- Aston-Jones, G. & Bloom, F.E. (1981). Activity of NE-containing locus coeruleus neurons in behaving rats anticipates fluctuations in the sleep-waking cycle. *J. Neurosci.*, 1, 876-886,
- Bobker, D.H. & Williams, J.T. (1989). Serotonin augments the cationic current  $I_h$  in central neurons. *Neuron*, 2, 1535-1540,
- Brand, A.; Behrend, O.; Marquardt, T.; McAlpine, D. & Grothe, B. (2002). Precise inhibition is essential for microsecond interaural time difference coding. *Nature*, 417, 543-547,
- Brugge, J.F. (1992). An overview of central auditory processing, In: *The mammalian auditory pathway: Neurophysiology*, Popper, A.N. & Fay, R.R., (Ed.), 1-33, Springer-Verlag, New York
- Burger, R.M.; Cramer, K.S.; Pfeiffer, J.D. & Rubel, E.W. (2005). Avian superior olivary nucleus provides divergent inhibitory input to parallel auditory pathways. *J. Comp. Neurol.*, 481, 6-18,
- Cant, N.B. & Hyson, R.L. (1992). Projections from the lateral nucleus of the trapezoid body to the medial superior olivary nucleus in the gerbil. *Hear. Res.*, 58, 26-34,
- Carr, C.E. & Konishi, M. (1988). Axonal delay lines for time measurement in the owl's brainstem. *Proc. Natl. Acad. Sci. USA*, 85, 8311-8315,
- Carr, C.E. & Konishi, M. (1990). A circuit for detection of interaural time differences in the brain stem of the barn owl. *J. Neurosci.*, 10, 3227-3246,
- Carr, C.E. & Boudreau, R.E. (1993). An axon with a myelinated initial segment in the bird auditory system. *Brain Res.*, 628, 330-334,
- Casseday, J.H. & Neff, W.D. (1973). Localization of pure tones. *J. Acoust. Soc. Am.*, 54, 365-372,
- Catterall, W.A. (1981). Localization of sodium channels in cultured neural cells. *J. Neurosci.*, 1, 777-783,
- Dasika, V.D.; White, J.A.; Carney, L.H. & Colburn, H.S. (2005). Effects of inhibitory feedback in a network model of avian brain stem. *J. Neurophysiol.*, 94, 400-411,
- DiFrancesco, D.; Ferroni, A.; Mazzanti, M. & Tromba, C. (1986). Properties of the hyperpolarizing-activated current ( $I_f$ ) in cells isolated from the rabbit sino-atrial node. *J. Physiol.*, 377, 61-88,
- DiFrancesco, D. & Tromba, C. (1988a). Inhibition of the hyperpolarization-activated current ( $I_f$ ) induced by acetylcholine in rabbit sino-atrial node myocytes. *J. Physiol.*, 405, 477-491,
- DiFrancesco, D. & Tromba, C. (1988b). Muscarinic control of the hyperpolarization-activated current ( $I_f$ ) in rabbit sino-atrial node myocytes. *J. Physiol.*, 405, 493-510,
- Finlayson, P.G. & Caspary, D.M. (1991). Low-frequency neurons in the lateral superior olive exhibit phase-sensitive binaural inhibition. *J. Neurophysiol.*, 65, 598-605,
- Fujita, I. & Konishi, M. (1991). The role of GABAergic inhibition in processing of interaural time difference in the owl's auditory system. *J. Neurosci.*, 11, 722-739,
- Fukui, I. & Ohmori, H. (2004). Tonotopic gradients of membrane and synaptic properties for neurons of the chicken nucleus magnocellularis. *J. Neurosci.*, 24, 7514-7523,
- Fukui, I.; Burger, R.M.; Ohmori, H. & Rubel E.W. (2010). GABAergic inhibition sharpens the frequency tuning and enhances phase locking in the chicken nucleus magnocellularis neurons. *J. Neurosci.*, 30, 12075-12083,

- Heffner, R.S. & Heffner, H.E. (1988). Sound localization and use of binaural cues by the gerbil (*Meriones unguiculatus*). *Behav. Neurosci.*, 102, 422-428,
- Jeffress, L.A. (1948). A place theory of sound localization. *J. Comp. Physiol. Psychol.*, 41, 35-39,
- Jones, B.E. & Moore, R.Y. (1977). Ascending projections of the locus coeruleus in the rat. II. Autoradiographic study. *Brain Res.*, 127, 25-53,
- Joris, P.X. & Yin, T.C. (1995). Envelope coding in the lateral superior olive. I. Sensitivity to interaural time differences. *J. Neurophysiol.*, 73, 1043-1062,
- Klump, G.M.; Windt, W. & Curio, E. (1986). The great tit's (*Parus major*) auditory resolution in azimuth. *J. Comp. Physiol.*, 158, 383-390,
- Klump, G.M. (2000). Sound localization in birds. In: *Comparative Hearing: Birds and Reptiles*, Dooling, R.J.; Fay, R.R. & Popper, A.N. (Eds.), 249-307, Springer, New York
- Knudsen, E.I. & Konishi, M. (1979). Mechanisms of sound localization in the barn owl (*Tyto alba*). *J. Comp. Physiol.*, 133, 13-21,
- Koch, U.; Braun, M.; Kapfer, C. & Grothe, B. (2004). Distribution of HCN1 and HCN2 in rat auditory brainstem nuclei. *Eur. J. Neurosci.*, 20, 79-91,
- Konishi, M. (2003). Coding of auditory space. *Annu. Rev. Neurosci.*, 26, 31-55,
- Kuba, H.; Koyano, K. & Ohmori, H. (2002). Development of membrane conductance improves coincidence detection in the nucleus laminaris of the chicken. *J. Physiol.*, 540, 529-542,
- Kuba, H.; Yamada, R. & Ohmori, H. (2003). Evaluation of the limiting acuity of coincidence detection in nucleus laminaris of the chicken. *J. Physiol.*, 552, 611-620,
- Kuba, H.; Yamada, R.; Fukui, I. & Ohmori, H. (2005). Tonotopic specialization of auditory coincidence detection in nucleus laminaris of the chick. *J. Neurosci.*, 25, 1924-1934,
- Kuba, H.; Ishii, T.M. & Ohmori, H. (2006). Axonal site of spike initiation enhances auditory coincidence detection. *Nature*, 444, 1069-1072,
- Lachica, E.A.; Rubsamen, R. & Rubel, E.W. (1994). GABAergic terminals in nucleus magnocellularis and laminaris originate from the superior olivary nucleus. *J. Comp. Neurol.*, 348, 403-418,
- Ludwig, A.; Zong, X.; Jeglitsch, M.; Hofmann, F. & Biel, M. (1998). A family of hyperpolarization-activated mammalian cation channels. *Nature*, 393, 587-591,
- Luscher, H.R. & Larkum, M.E. (1998). Modeling action potential initiation and back-propagation in dendrites of cultured rat motoneurons. *J. Neurophysiol.*, 80, 715-729,
- Mainen, Z.F.; Foerger, J.; Huguenard, J.R. & Sejnowski, T.J. (1995). A model of spike initiation in neocortical pyramidal neurons. *Neuron*, 15, 1427-1439,
- Manley, G.A.; Koppl, C. & Konishi, M. (1988). A neural map of interaural intensity differences in the brain stem of the barn owl. *J. Neurosci.*, 8, 2665-2676,
- Masterton, B.; Thompson, G.C.; Bechtold, J.K. & RoBards, M.J. (1975). Neuroanatomical basis of binaural phase-difference analysis for sound localization: a comparative study. *J. Comp. Physiol. Psychol.*, 89, 379-386,
- Mills, A.W. (1958). On the minimum audible angle. *J. Acoust. Soc. Am.*, 30, 237-246,
- Mogdans, J. & Knudsen, E.I. (1994). Representation of interaural level difference in the VLVp, the first site of binaural comparison in the barn owl's auditory system. *Hear. Res.*, 74, 148-164,
- Moiseff, A. & Konishi, M. (1981). Neuronal and behavioral sensitivity to binaural time differences in the owl. *J. Neurosci.*, 1, 40-48,



- Moiseff, A. & Konishi, M. (1983). Binaural characteristics of units in the owl's brainstem auditory pathway: precursors of restricted spatial receptive fields. *J. Neurosci.*, 3, 2553-2562,
- Monsivais, P.; Yang, L. & Rubel, E.W. (2000). GABAergic inhibition in nucleus magnocellularis: implications for phase locking in the avian auditory brainstem. *J. Neurosci.*, 20, 2954-2963,
- Nishino, E.; Yamada, R.; Kuba, H.; Hioki, H.; Furuta, T.; Kaneko, T. & Ohmori, H. (2008). Sound-intensity-dependent compensation for the small interaural time difference cue for sound source localization. *J. Neurosci.*, 28, 7153-7164,
- Oertel, D. (1999). The role of timing in the brain stem auditory nuclei of vertebrates. *Annu. Rev. Physiol.*, 61, 497-519,
- Overholt, E.M.; Rubel, E.W. & Hyson, R.L. (1992). A circuit for coding interaural time differences in the chick brainstem. *J. Neurosci.*, 12, 1698-1708,
- Pape, H.C. (1996). Queer current and pacemaker: the hyperpolarization-activated cation current in neurons. *Annu. Rev. Physiol.*, 58, 299-327,
- Park, T.J. & Dooling, R.J. (1991). Sound localization in small birds: absolute localization in azimuth. *J. Comp. Psychol.*, 105, 125-133,
- Parks, T.N. (2000). The AMPA receptors of auditory neurons. *Hear. Res.*, 147, 77-91,
- Pecka, M.; Brand, A.; Behrend, O. & Grothe, B. (2008). Interaural time difference processing in the mammalian medial superior olive: the role of glycinergic inhibition. *J. Neurosci.*, 28, 6914-6925,
- Pena, J.L.; Viete, S.; Albeck, Y. & Konishi, M. (1996). Tolerance to sound intensity of binaural coincidence detection in the nucleus laminaris of the owl. *J. Neurosci.*, 16, 7046-7054,
- Rathouz, M. & Trussell, L.O. (1998). Characterization of outward currents in neurons of the avian nucleus magnocellularis. *J. Neurophysiol.*, 80, 2824-2835,
- Reyes, A.D.; Rubel, E.W. & Spain, W.J. (1996). In vitro analysis of optimal stimuli for phase-locking and time-delayed modulation of firing in avian nucleus laminaris neurons. *J. Neurosci.*, 16, 993-1007,
- Rosenberger, M.H.; Fremouw, T.; Casseday, J.H. & Covey, E. (2003). Expression of Kv1.1 ion channel subunit in the auditory brainstem of the big brown bat, *Eptesicus fuscus*. *J. Comp. Neurol.*, 462, 101-120,
- Rubel, E.W. & Parks, T.N. (1975). Organization and development of the brain stem auditory nuclei of the chicken: tonotopic organization of N. magnocellularis and N. laminaris. *J. Comp. Neurol.*, 164, 411-434,
- Santoro, B.; Liu, D.T.; Yao, H.; Bartsch, D.; Kandel, E.R.; Siegelbaum, S.A. & Tibbs, G.R. (1998). Identification of a gene encoding a hyperpolarization-activated pacemaker channel of brain. *Cell*, 93, 717-729,
- Santoro, B. & Tibbs, G.R. (1999). The HCN gene family: molecular basis of the hyperpolarization-activated pacemaker channels. *Ann. N.Y. Acad. Sci.*, 868, 741-764,
- Sato, T.; Fukui, I. & Ohmori, H. (2010). Interaural phase difference modulates the neural activity in the nucleus angularis and improves the processing of level difference cue in the lateral lemniscal nucleus in the chicken. *Neurosci. Res.*, 66, 198-212,
- Scheibel, M.E. & Scheibel, A.B. (1974). Neuropil organization in the superior olive of the cat. *Exp. Neurol.*, 43, 339-348,

- Scott, L.L.; Mathews, P.J. & Golding, N.L. (2005). Posthearing developmental refinement of temporal processing in principal neurons of the medial superior olive. *J. Neurosci.*, 25, 7887-7895,
- Smith, A.J.; Steven, O. & Forsythe, I.D. (2000). Characterization of inhibitory and excitatory postsynaptic currents of the rat medial superior olive. *J. Physiol.*, 529, 681-698,
- Smith, P.H.; Joris, P.X. & Yin, T.C. (1993). Projections of physiologically characterized spherical bushy cell axons from the cochlear nucleus of the cat: evidence for delay lines to the medial superior olive. *J. Comp. Neurol.*, 331, 245-260,
- Smith, P.H. (1995). Structural and functional differences distinguish principal from nonprincipal cells in the guinea pig MSO slice. *J. Neurophysiol.*, 73, 1653-1667,
- Spangler, K.M.; Warr, W.B. & Henkel, C.K. (1985). The projections of principal cells of the medial nucleus of the trapezoid body in the cat. *J. Comp. Neurol.*, 238, 249-262,
- Sullivan, W.E. & Konishi, M. (1984). Segregation of stimulus phase and intensity coding in the cochlear nucleus of the barn owl. *J. Neurosci.*, 4, 1787-1799,
- Svirskis, G.; Kotak, V.; Sanes, D.H. & Rinzel, J. (2002). Enhancement of signal-to-noise ratio and phase locking for small inputs by a low-threshold outward current in auditory neurons. *J. Neurosci.*, 22, 11019-11025,
- Takahashi, T.; Moiseff, A. & Konishi, M. (1984). Time and intensity cues are processed independently in the auditory system of the owl. *J. Neurosci.*, 4, 1781-1786,
- Takahashi, T.T. & Konishi, M. (1988). Projections of nucleus angularis and nucleus laminaris to the lateral lemniscal nuclear complex of the barn owl. *J. Comp. Neurol.*, 274, 212-238,
- Tollin, D.J. & Yin, T.C. (2005). Interaural phase and level difference sensitivity in low-frequency neurons in the lateral superior olive. *J. Neurosci.*, 25, 10648-10657,
- Trussell, L.O. (1999). Synaptic mechanisms for coding timing in auditory neurons. *Annu. Rev. Physiol.*, 61, 477-496,
- Warchol, M.E. & Dallos, P. (1990). Neural coding in the chick cochlear nucleus. *J. Comp. Physiol. A*, 166, 721-734,
- Yamada, R.; Kuba, H.; Ishii, T.M. & Ohmori, H. (2005). Hyperpolarization-activated cyclic nucleotide-gated cation channels regulate auditory coincidence detection in nucleus laminaris of the chick. *J. Neurosci.*, 25, 8867-8877,
- Yang, L.; Monsivais, P. & Rubel, E.W. (1999). The superior olivary nucleus and its influence on nucleus laminaris: a source of inhibitory feedback for coincidence detection in the avian auditory brainstem. *J. Neurosci.*, 19, 2313-2325,
- Yin, T.C. (2002). Neural Mechanisms of Encoding Binaural Localization Cues in the Auditory Brainstem. In: *Integrative Functions in the Mammalian Auditory Pathway*, Oertel, D, (Ed), 99-159, Springer-Verlag, New York
- Young, S.R. & Rubel, E.W. (1983). Frequency-specific projections of individual neurons in chick brainstem auditory nuclei. *J. Neurosci.*, 3, 1373-1378,



## **Advances in Sound Localization**

Edited by Dr. Pawel Strumillo

ISBN 978-953-307-224-1

Hard cover, 590 pages

**Publisher** InTech

**Published online** 11, April, 2011

**Published in print edition** April, 2011

Sound source localization is an important research field that has attracted researchers' efforts from many technical and biomedical sciences. Sound source localization (SSL) is defined as the determination of the direction from a receiver, but also includes the distance from it. Because of the wave nature of sound propagation, phenomena such as refraction, diffraction, diffusion, reflection, reverberation and interference occur. The wide spectrum of sound frequencies that range from infrasounds through acoustic sounds to ultrasounds, also introduces difficulties, as different spectrum components have different penetration properties through the medium. Consequently, SSL is a complex computation problem and development of robust sound localization techniques calls for different approaches, including multisensor schemes, null-steering beamforming and time-difference arrival techniques. The book offers a rich source of valuable material on advances on SSL techniques and their applications that should appeal to researches representing diverse engineering and scientific disciplines.

### **How to reference**

In order to correctly reference this scholarly work, feel free to copy and paste the following:

Rei Yamada and Harunori Ohmori (2011). Frequency Dependent Specialization for Processing Binaural Auditory Cues in Avian Sound Localization Circuits, *Advances in Sound Localization*, Dr. Pawel Strumillo (Ed.), ISBN: 978-953-307-224-1, InTech, Available from: <http://www.intechopen.com/books/advances-in-sound-localization/frequency-dependent-specialization-for-processing-binaural-auditory-cues-in-avian-sound-localization>

**INTECH**  
open science | open minds

### **InTech Europe**

University Campus STeP Ri  
Slavka Krautzeka 83/A  
51000 Rijeka, Croatia  
Phone: +385 (51) 770 447  
Fax: +385 (51) 686 166  
[www.intechopen.com](http://www.intechopen.com)

### **InTech China**

Unit 405, Office Block, Hotel Equatorial Shanghai  
No.65, Yan An Road (West), Shanghai, 200040, China  
中国上海市延安西路65号上海国际贵都大饭店办公楼405单元  
Phone: +86-21-62489820  
Fax: +86-21-62489821

© 2011 The Author(s). Licensee IntechOpen. This chapter is distributed under the terms of the [Creative Commons Attribution-NonCommercial-ShareAlike-3.0 License](https://creativecommons.org/licenses/by-nc-sa/3.0/), which permits use, distribution and reproduction for non-commercial purposes, provided the original is properly cited and derivative works building on this content are distributed under the same license.

IntechOpen

IntechOpen